Mansoura Engineering Journal

Volume 49 | Issue 2 Article 1

2023

Efficient Design and Implementation of Miniaturized Microstrip Diplexer Using Dual Open Stub Loaded Resonator for 5G Applications

Islam F. Abu Elkhair
Researcher at Electronics and Communications Engineering Department, Mansoura University, Mansoura, Egypt., eng.islamfawzi226@gmail.com

Hamdi A. Elmikati
Professor at the Electronics and Communications Engineering Department, Mansoura University, Mansoura, Egypt

Mohamed M. Ashour
Associate Professor at Electronics and Communications Engineering Department, Faculty of Engineering, Mansoura University, Mansoura, Egypt.

Amr H. Hussein
Professor of antennas, Electronics and Electrical Communications Engineering Department. Faculty of Engineering. Tanta University, Tanta, Egypt.

ORIGINAL STUDY

Efficient Design and Implementation of Miniaturized Microstrip Diplexer Using Dual-Open Stub-Loaded Resonator for 5G Applications

Islam F. Abu Elkhair [a,*], Hamdi A. Elmikati [a], Mohamed M. Ashour [b], Amr H. Hussein [c,d]

[a] Department of Electronics and Communications Engineering, Mansoura University, Egypt
[b] Department of Electronics and Communications Engineering, Faculty of Engineering, Mansoura University, Mansoura, Egypt
[c] Department of Electronics and Electrical Communications Engineering, Faculty of Engineering, Tanta University, Tanta, Egypt
[d] Department of Electronics and Electrical Communications Engineering, Faculty of Engineering, Horus University, New Damietta, Egypt

Abstract

The design and implementation of a compact size diplexer with high isolation, low insertion loss, and small fractional bandwidths is a promising issue in recent wireless communication systems. In this paper, a novel microstrip diplexer has been introduced based on the utilization of the dual open stub loaded resonator technique. The proposed design has a very compact size of with a high operating power efficiency. The diplexer is designed to operate at two resonance frequencies of and with very low insertion losses of and, respectively. Moreover, it provides high isolation values of and for and, respectively. The diplexer provides high selectivity as the fractional bandwidths were settled at and for each channel, respectively. Furthermore, an acceptable agreement between the simulation results and the fabrication measurements of the proposed diplexer is achieved. The operating characteristics allow the structure for many applications of ultrawideband, however mainly it is suitable for 5G communication systems.

Keywords: Bandpass filter, Diplexer, Dual-open stub-loaded resonator, Dual stub resonator, Microstrip antenna

1. Introduction

In the last few years, wireless communication systems have revolutionized the way we connect and communicate in today's digital age. From smartphones and Wi-Fi networks to satellite communications and Bluetooth devices, wireless technology has become an integral part of our daily lives, offering convenience, mobility, and increased connectivity. With the rapid growth of mobile generations and with 5 G (fifth generation) technology which is the fastest growing mobile technology in history, promises faster data speeds, lower latency, and increased network capacity, unlocking new possibilities for applications like autonomous vehicles, smart cities, and immersive virtual reality experiences. Therefore, expected to be a sharp increase in transmitting much more data with the existence of more available bandwidth and advanced antenna technology.

The key component of frequency division duplex technology is a microwave diplexer. It is a passive microwave device integrated with a transceiver and has many applications in modern high-speed wireless antenna systems, which consists of two filters for transmission and reception that are connected by a matching network. In the differential frequency duplex systems, the diplexer is located in the front-end RF circuit connected with a transceiver antenna, which can both isolate the received and transmitted signals, while ensuring that the microwave system can transmit typically simultaneously (Zhou et al.,

Received 16 August 2023; revised 13 October 2023; accepted 23 October 2023.
Available online 30 November 2023

* Corresponding author. Mansoura, Egypt.
E-mail address: Eng.islamfawzi226@gmail.com (I.F. Abu Elkhair).

https://doi.org/10.58491/2735-4202.3131

2023). This allows them to operate separately without interfering with one another.

In this context, multiplexers and diplexers are key components in many microwave communication systems (Tahmasbi et al., 2021; Hammed, 2022), such as radar systems, cellular phones, satellite communication systems, and broadcast stations are usually used at multiple frequencies. A diplexer may be used to combine the signals and use a single antenna to broadcast. Therefore, the use of the same antenna for multiple frequencies is the main point of designing a diplexer (Chinig and Bennis, 2017), and hence it helps to less space requirements for the whole structure antenna and reduces the system's overall cost. When designing an RF diplexer there are many factors to consider. The most critical thing is the degree of isolation or rejection required between the ports of transmitter/receiver frequencies, which is a complex task with a matching network which provides high attenuation in another pass band. Many techniques have been known for years to design a diplexer layout. The most common technique is the open loop resonator whether U-shaped or T-shaped (Chuang and Wu, 2011), which greatly helps to high isolation and then reduces losses. All methods have been proposed generally combining two bandpass filters (BPFs) (Gorur et al., 2022) to lets only the frequency of a required range pass. BPFs are commonly installed on a dielectric substrate and can give more flexibility to the circuit layout.

As a result of the importance of diplexer for 5 G networks and all future generations, all the research that has been done recently seeking to develop a high-performance electrical diplexer requested to operate in multiband mobile communication systems, having a compact size, very high degree of isolation, excellent frequency selectivity, low insertion loss (IL), wide stop band, and low cost. The dual closed-loop stepped impedance resonator is used to minimize the diplexer size; however, it offers poor signal isolation (worse than 27 dB) (Dembele et al., 2019). To reach a high degree of isolation between channels based on the low-pass dual-BPFs, but seemed not good enough (worse than 21 dB) (Bavandpour et al., 2021). The interdigital coupled lines and stepped-impedance circuit are used to introduce a low-loss microstrip diplexer; however, frequency selectivity must be considered more (Bui et al., 2017). In Chinig et al. (2014), a diplexer design based on an asymmetric fork-form feed line and open-loop resonators to enhance out-of-band rejection is considered, but the IL needs more improvement. In Yang et al. (2019), the proposed diplexer design seeks to produce a very high-performance function, but in return, the size of the final structure is very high and will be expensive. New octagonal resonators are used to achieve a compact microstrip diplexer in Ben Haddi et al. (Ben Haddi et al., 2023); nevertheless, they suffer from high ILs and a low isolation of about 25 dB. The mentioned diplexers are presented in the past. All structures have many disadvantages such as high IL, poor isolation, low performance, and a large size, which mean more components and therefore high cost.

In this paper, a novel method of mutual coupling for a compact microstrip diplexer has been presented having high performance and an unprecedented degree of IL. Initially, the proposed function is made up of two compact-size BPFs that are matched to the transceiver antenna connected by a matching network which works as a combining circuit, resulting in a very good degree of isolation between the received and transmitted signals calculated by 35 and 60 dB based on a dual-open stub-loaded resonator (DOSLR). A high selectivity BPF is created for 8.4 GHz operation. The suggested microstrip diplexer is then made up of the other BPF, which is created to operate at 10.8 GHz supported wireless communication systems and 5 G applications. Therefore, this work introduces a high isolation and low IL effective design scheme for microstrip diplexers. The two compact-size BPFs that make up the proposed diplexer are constructed from linked DOSLR. A T-junction that serves as a combining circuit connects the two BPFs to the antenna and provides good isolation between the uplink and downlink BPFs. The S-parameter results on ADS software were tested and compared with another simulator program computer simulation technology (CST) Microwave Studio and it turned out that a great convergence was achieved between them. The structure of this paper is as follows. The microstrip diplexers design process is described in Section 2. The fabrication and measurements are discussed in Section 3. Section 4 presents a comparison with past works. The paper is concluded in Section 5.

2. Proposed diplexer

In this section, the design of a three-port diplexer with a novel structure based on DOSLR is explained and simulated. The diplexer that allows dual resonance bands 8.4 and 10.8 GHz has many features compared with others as it is distinguished with very compact size, very low IL, and very high isolation power thanks to the DOSLR based on the dual BPF technique. The design provides propagation in ultra-wideband as it is supposed to be used in wireless applications and new 5 G applications. The proposed structure is aimed to design on a

Rogers substrate of type TMM4 that has a height of $h = 1.52\ mm$ and a dielectric constant of $\varepsilon r = 4.5$. The design will be simulated on the CST program and it is LC equivalent circuit of BPF will be designed and tested on the ADS program to compare the final results. The section procedure will be moved as follows:

(1) Design of the DOSLR resonator.
(2) Design of BPF and equivalent LC circuit.
(3) Proposed layout design and its simulation results.

2.1. Design of the dual-open stub-loaded resonator resonator

One of the most popular techniques of topology for designing microstrip Chips such as antennas, filters, and diplexers is the open stub resonator. It is named also in many researches as the U-shaped resonator for the reason that its shape construction is tucked from its edge and contains a gap from one of its edges. Due to its many features compared with other techniques such as its very concise tiny size structure as well as its versatility in many different functions and its high isolation for microstrip diplexers, the open stub resonator is used in the proposed structure with an improvement to be dual structure around the capacitance to increase the isolation of the diplexer using loaded fingers to increase the load capacitance in the structure as shown in Fig. 1.

DOSLR is composed of two-folded straight lines shunted with fingers for each side; moreover, the capacitance effect is present because of the gap located between port 1 and port 2 feed lines. The use of asymmetric feed lines between port 2 and port 3 is chosen in the design to enhance the stop band filter by presenting that the transmission zeros in the two ports are very close and also in the pass band, and thus the BPF selects the frequency band easily.

The equivalent transmission model is introduced in Fig. 1b. The electrical length of the resonator transmission line is presented by $\theta_T = \theta_1 + \theta_2$, where θ_1, θ_2 represent the length of the short and long ways for the resonator from the input transmission line. Furthermore, it could be assumed lossless transmission so that Z_{in} could be expressed as in equation (1) (Chinig et al., 2014):

$$Z_{in} = \frac{Z_0}{j\,\tan g(\theta)} \tag{1}$$

Note that Z_{in} expresses the input impedance; Z_0 expresses the characteristic impedance for the structure; and finally θ represents the transmission line electrical length.

However, the analysis of admittance could be expressed using expressions (2) and (3) (Chinig et al., 2014):

$$Y_{in} = Y_{in1} + Y_{in2} \tag{2}$$

$$Y_{in} = \frac{1}{Z_{in1}} + \frac{1}{Z_{in2}} = \frac{1}{\frac{Z_0}{j\,\tan g(\theta_1)}} + \frac{1}{\frac{Z_0}{j\,\tan g(\theta_2)}} \tag{3}$$

Note that Y_{in} is the input impedance, the final equation could be expressed by (4) (Chinig et al., 2014):

$$Y_{in} = jY_0[\tan(\theta_1) + \tan(\theta_2)] = jY_0\frac{\mathrm{Sin}(\theta_T)}{\cos(\theta_1)\cos(\theta_2)} \tag{4}$$

It is known that the resonance frequency of the structure occurred at $\theta_T = n\pi$ or $l = n\lambda/2$; however, the standing wave always operates at $Y_{in} = 0$. Moreover, we conclude that voltage reaches its maximum value when the open edges of the resonator impose the current to be zero.

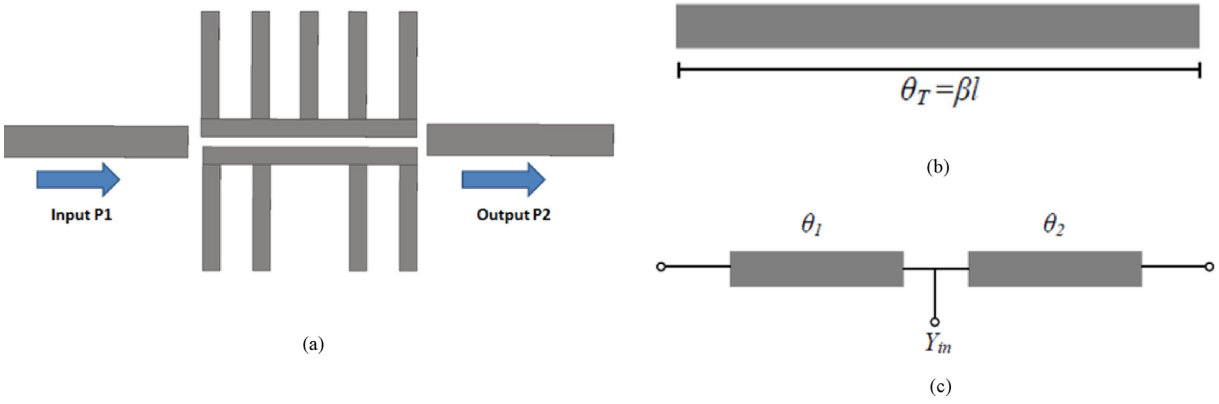

Fig. 1. (a) The proposed dual–open-loaded stub resonator (DOSLR), (b) line resonator, and (c) equivalent circuit of line resonator.

2.2. Design of bandpass filter and equivalent LC circuit

It is known that the design of any microstrip diplexer depends on the configuration of the filter. So that, there are many designs that depend on the integration of a high pass filter with a low pass filter. Otherwise, some designs depend on the connection between a BPF with a band stop filter to achieve the desired propagation band. The proposed DOSLR mainly depends on the integration between two BPFs, which is the most common construction used in the design of microstrip diplexers. The proposed filters are designed to transmit and receive the propagation bands at 8.4 and 10.8 GHz, respectively.

Assuming that the waveguide length is represented by λ g, for the sake of the compact dimension λ g/4, the choice of DOSLR was the best utilized design for the proposed structure. First of all, the proposed DOSLR used for designing the two BPFs consists of two mutual magnetic coupling DOSLR each of which is parallel to the feed line. The mutual coupling between input and output feed lines is controlled by a gap between them. The DOSLR cell is supported by fingers on each side to increase the isolation from IL. The BPF structure is designed on a Rogers TMM4 substrate with height $h = 1.5mm$ and dielectric constant $\varepsilon_r = 4.5$. Fig. 2 shows the dimensions of the proposed BPF. The parameter Wr2 = 0.5 mm represents the width of the fingers, as well as Lr5 = 0.9 mm represents the gaps between upper fingers; moreover, Lr6 = 2.2 mm represents the middle gap between the lower fingers, finally Lr7 = 0.2 mm represents the internal mutual gap between the two feed lines of the BPF. However

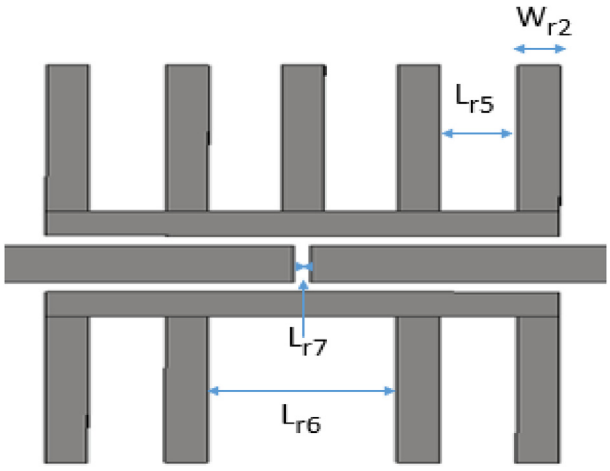

Fig. 2. Configuration of the DOSLR-based BPF. BPF, bandpass filter; DOSLR, dual-open stub-loaded resonator.

Fig. 3 shows the simulation results of the scattering parameters of the filter. The resonance frequency of the filter is centered at 8.4*GHz*. The parameter S11 which clarifies that input reflection coefficient is below −18 dB; S21 the reverse transmission of the filter tends to zero; and eventually the isolation of the circuit tends to 35 dB, which are very accepted results.

In the microwave study, the topology of converting the structure design to an LC circuit has become very necessary to understand the behavior of the design and to form a complete proof of the final results, so this section will present a clear picture of the LC equivalent circuit. Fig. 4 shows the equivalent LC circuit model of the BPF generated by the ADS program. The values of the circuit parameters including inductance and capacitance are listed in Tables 1 and 2, respectively.

Assume that the microstrip feed lines and the fingers of resonators are all lossless material to facilitate the analysis of the LC equivalent circuit. The transmission feed lines and the finger inductances are represented in L_1, L_2 , L_3, L_4, L_5, L_6, L_7 , L_8 , L_9, L_{10}, L_{11}, L_{12}, L_{13} .However, the gap between the transmission lines is represented by C1; the gap between the transmission lines and the resonators lines is represented by C2, C3, C4, and C5. The capacitance effect that engenders the finger stubs and the ground is represented by C13, C14, C23, and C24. Finally, C6, C7, C8, C9, C10, C11, C12, C15, C16, C17, C18, C19, C20, C21, and C22, are the capacitance effect of the bends of the DOSLR cell and between the shunt fingers.

To analyze the circuit parameters, equations (5) and (6) are used to calculate the inductance or capacitance of the circuit (Chinig and Bennis, 2017):

$$\mathrm{L} = \mathrm{C} Z_c V_p \tag{5}$$

$$\mathrm{L} = \frac{L\, V_p}{Z_c} \tag{6}$$

where L and C represent the capacitance and inductance of the structure; V_P represents the phase velocity and Zc represents the characteristic impedance of the circuit. Equations (7) and (8) are used to determine the values of Zc and V_P (Chinig and Bennis, 2017):

$$\mathrm{V_P} = \frac{\mathrm{C}}{\sqrt{\varepsilon_{\mathrm{re}}}} \tag{7}$$

$$Z_c = \frac{\eta}{2\pi\sqrt{\varepsilon_{re}}} \mathrm{In}\left[8\frac{h}{W} + 0.25\frac{W}{h}\right] \tag{8}$$

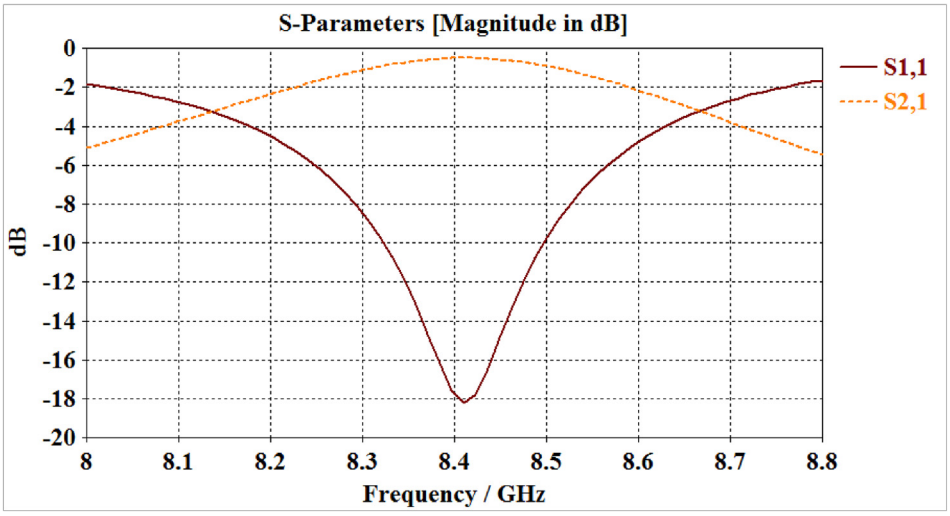

Fig. 3. Simulation of scattering parameters of the DOSLR-based BPF. BPF, bandpass filter; DOSLR, dual-open stub-loaded resonator.

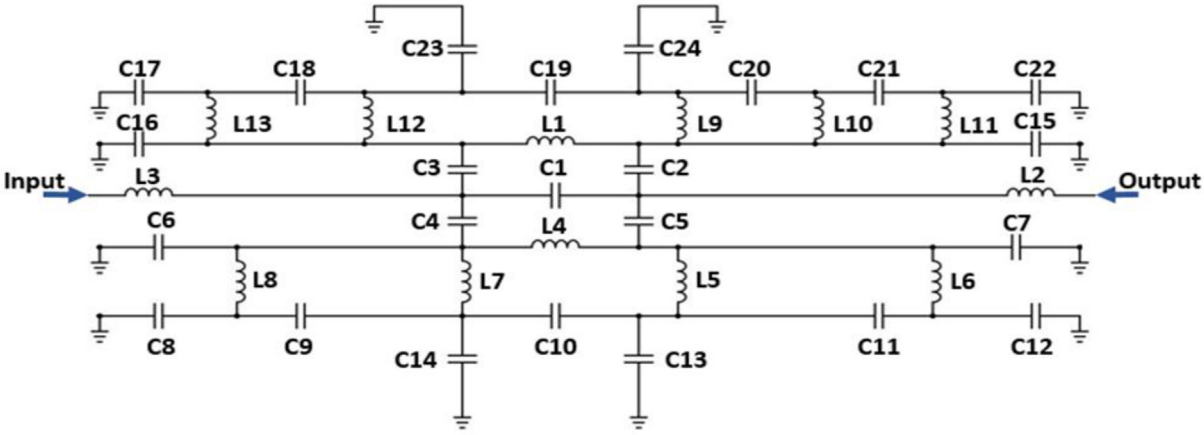

Fig. 4. LC model of BPF that represents the DOSLR circuit. BPF, bandpass filter; DOSLR, dual-open stub-loaded resonator.

Table 1. Values of inductance components used in circuit simulation (all in nH).

L1	L2	L3	L4	L5	L6	L7	L8	L9	L10	L11	L12	L13
3.45	1.57	1.57	3.13	0.85	0.85	0.85	0.85	1.8	1.8	1.8	1.8	1.8

where ε_{re} is the dielectric permittivity that can be calculated using equation (9) (Chinig and Bennis, 2017):

$$\varepsilon_{re}=\frac{\varepsilon_r+1}{2}+\frac{\varepsilon_r-1}{2}\left\{\left(1+12\frac{h}{W}\right)^{-0.5}+0.04\left(1-\frac{W}{h}\right)^{2}\right\} \tag{9}$$

The ADS simulator is used to construct the analogous LC circuit, and the results of the ADS and the CST are compared as shown in Fig. 5. This graph demonstrates a good correlation between the responses.

2.3. Proposed layout design and its simulation results

The layout of the proposed diplexer is shown in Fig. 6. It consists of two integrated BPFs tuned at two distinct frequencies. The dimensions of the proposed diplexer are: Wf0 = 1.40 mm, Wf1 = 0.75 mm, Wf2 = 0.75 mm, Wr1 = 0.50 mm, Wr2 = 0.50 mm, Lr1 = 9.0 mm, Lr2 = 6.0 mm, Lr3 = 20.5 mm, and Lr4 = 15.9 mm. The main design is based on two corresponding cells in each feed line as shown in Fig. 6. Each cell provides the gap of mutual inductance between the feed lines with suitable isolation to decrease the losses between the input port and

Table 2. Values of capacitive components used in circuit simulation (all in pF).

C1	C2	C3	C4	C5	C6	C7	C8	C9	C10	C11	C12
0.09	0.22	0.22	0.22	0.22	0.042	0.042	0.3	0.3	0.017	0.3	0.3
C13	C14	C15	C16	C17	C18	C19	C20	C21	C22	C23	C24
0.14	0.14	0.02	0.02	0.074	0.074	0.017	0.065	0.065	0.065	0.14	0.14

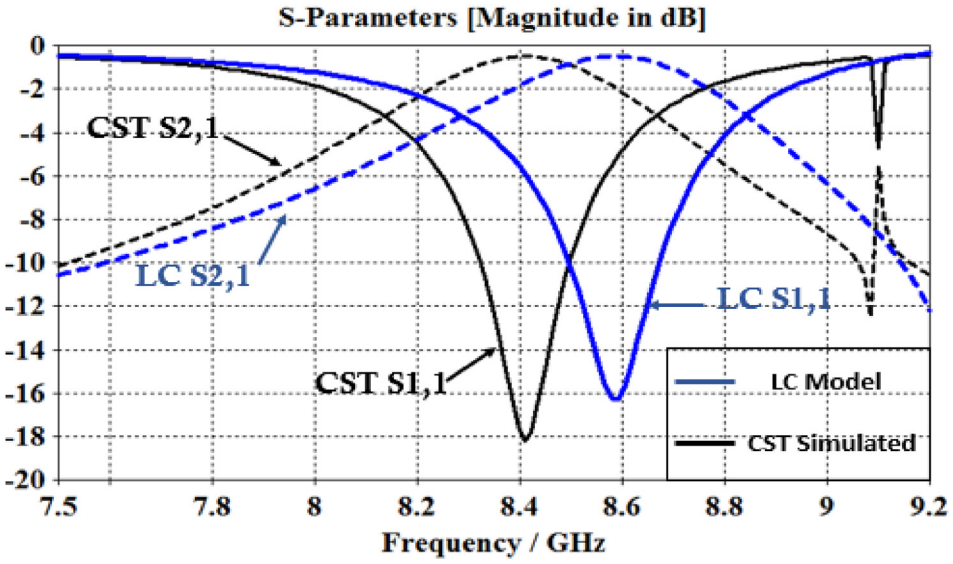

Fig. 5. A comparison between the ADS circuit model and the simulated CST design of the proposed BPF. BPF, bandpass filter; CSF, computer simulation technology.

the two output executors. The cells are designed by the DOSLR technique, which provides the structure with compactness in size as it is measured $(20.5 \times 15.9)mm^2$. The proposed structure is designed on a Rogers substrate of type TMM4 that has a height of $h = 1.52mm$ and a dielectric constant of $\varepsilon_r = 4.5$. The dual-loaded fingers support the design to operate in dual bands at center frequencies of 8.4 and 10.8 GHz, which makes it suitable for the applications of 5 G communication systems. However, the

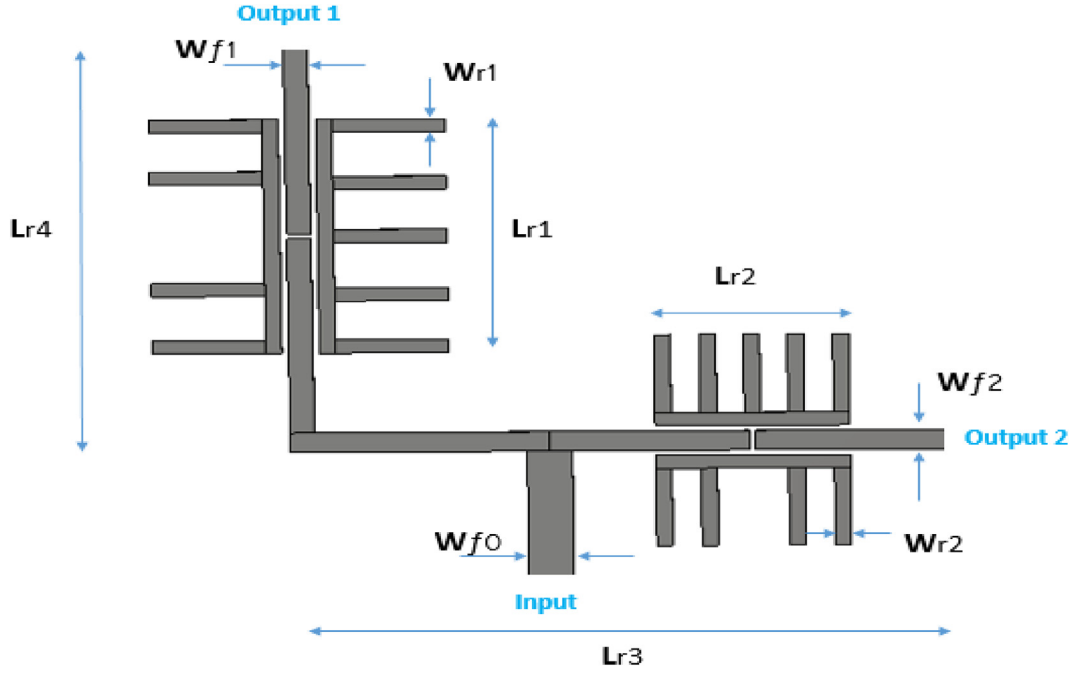

Fig. 6. Layout of the proposed diplexer structure.

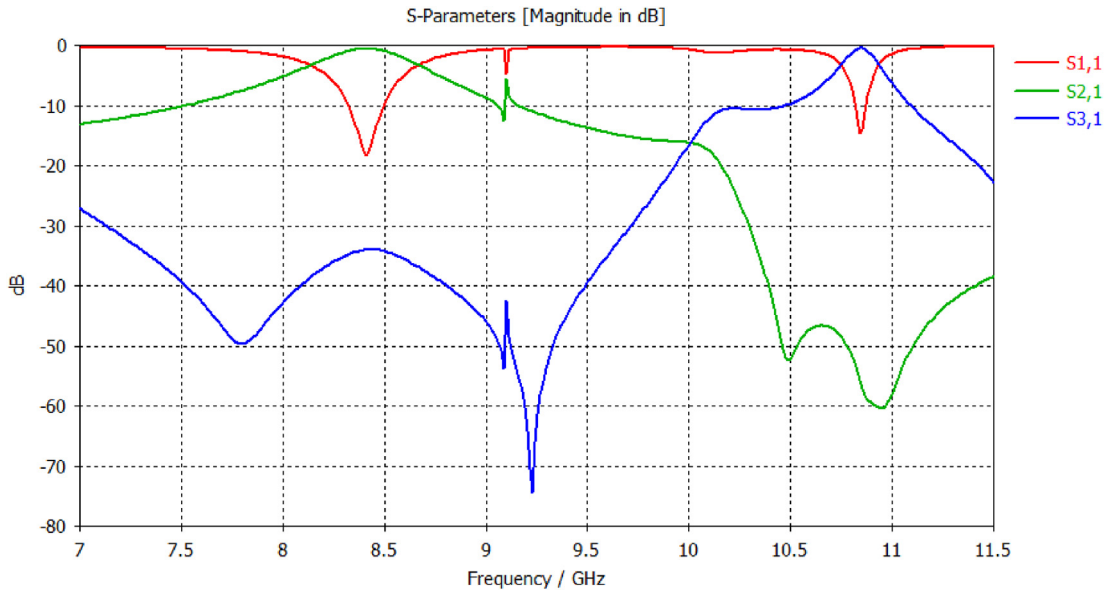

Fig. 7. Simulation of scattering parameters of the proposed diplexer.

structure exhibits highly favorable simulation results, with very low reflection losses of around −20 dB and low ILs of 0.43 and 0.33 dB at 8.4 and 10.8 GHz, respectively. Moreover, the transmission and receiving bands' bandwidths are 0.17 and 0.05 GHz, respectively. As demonstrated in Fig. 7, it further offers excellent isolation values of 35 and 60 dB at 8.4 and 10.8 GHz, respectively. Also, it provides a small fractional bandwidth of 2 and 4 % for each band.

3. Fabrication and measurements

The propound diplexer is fabricated on a Rogers TMM4 substrate with dielectric constant εr = 4.5 and thickness h = 1.52 mm. The fabricated structure area has a dimension of 20.5 × 15.9 mm^2 as shown in Fig. 8. The S-parameters of the fabricated structure were measured in lap by the Rohde and Schwarz ZVB 20 Network Analyzer. The comparison between the measured and simulated results is presented in Fig. 9. It shows a high match between them. The measurements are highlighted by the dashed lines to present ILs of 0.45 and 0.4 dB and the return losses are 17.5 and 16 dB at 8.4 and 10.8 GHz, respectively, as shown in Fig. 9. Also, it shows a comparison between the measured and simulated isolation at the two bands as the measured isolation values are 32 and 35 dB, which are highly matched with the simulation results.

4. Comparison with past works

In this section, a comparison between the proposed design and state-of-the-art works is introduced. Through this comparison, the benefits and precedence of the proposed diplexer will be clarified, as shown in Table 3. The fabricated design is characterized by a very high percent of isolation compared

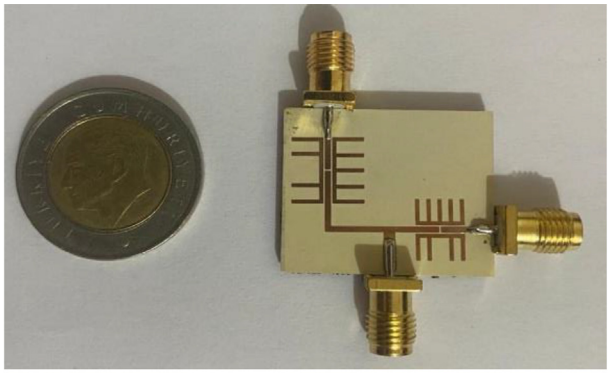

(a)

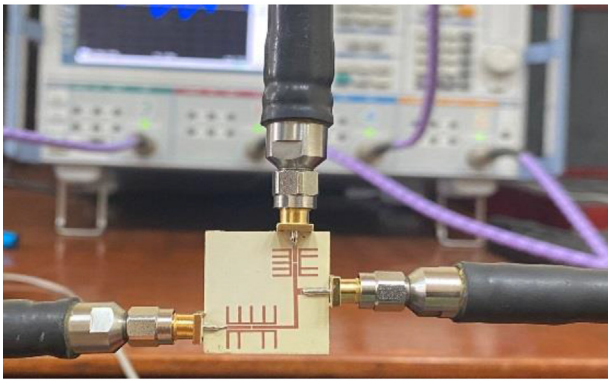

(b)

Fig. 8. Photograph of the fabricated diplexer: (a) top view and (b) S-parameter measurement.

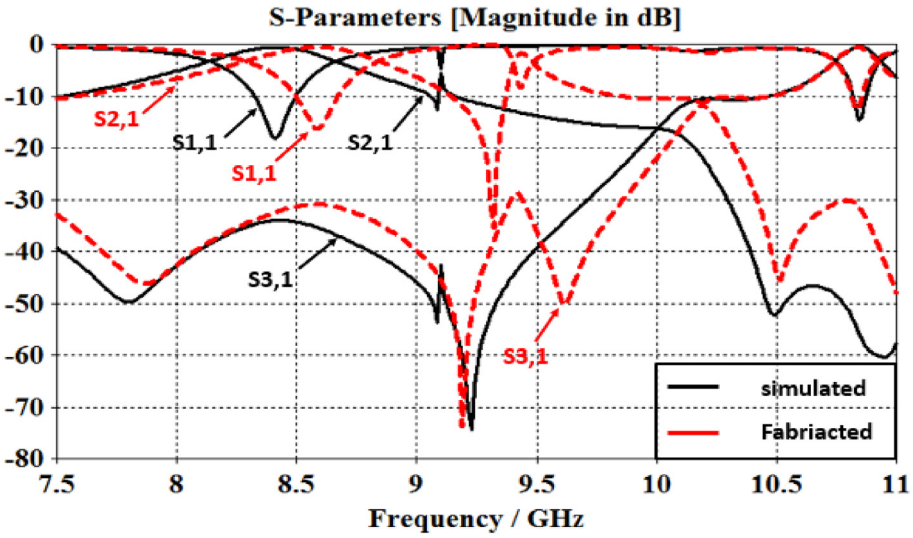

Fig. 9. Comparison between simulated and measured scattering parameters of the proposed diplexer.

Table 3. Comparison of the proposed diplexer with state-of-the-art works.

Diplexer	Frequency (GHz)	Fractional bandwidth (%)	Insertion loss (dB)	Isolation (dB)	Circuit size (mm^2)
Wu et al. (2022)	2.5/5.8	NA	1.67/1.58	>27	14.6 × 10.4
Chaudhary et al. (2023)	2.1/5.1	14.3/4	0.4/1.5	40	28.5 × 23.0
Roshani et al. (2023)	1.9/3.6	NA	0.55/0.87	>32	11.2 × 32.2
Song et al.	1.85/2.4	NA	0.8/1.5	>37	NA
Farah et al. (2022)	1.8/2.5	10.5/7.6	2.7/2.8	>18	47.40 × 247.0
Alnagar et al. (2022)	1.82/2.0	3.2/3.0	1.1/1.2	35/45	80 × 50
Haddi et al. (2022)	2.3/4.2	NA	2.2/1.9	60	34 × 32
Zhang et al. (2021)	4.3/8.75	50/51.4	2.3/3.0	25	NA
Hassan et al. (2021)	2.1/2.6	4/4	1.4/1.3	>40	30 × 60
Chinig et al. (2016)	5.8/3.17	8.9/9.75	1.86/2	>25	24 × 22
This work	8.4/10.8	2/4	0.43/0.33	35/60	20.5 × 15.9

with all other works, except for Alnagar et al. (2022) and Haddi et al. (2022), which has the same degree of isolation as the IL shows an unprecedented rate in this aspect with all results without exception. In another context, the frequency band in the proposed diplexer is higher than all, which can easily work in 5 G applications and wireless communication systems. High selectivity was also achieved in the proposed diplexer to a very acceptable degree except for that in Chaudhary et al. (2023) and Alnagar et al. (2022), which have precedence in this regard, but in return, they have high IL. The size of the proposed diplexer seems smaller and more effective in communication devices compared with the other designs except for Wu et al. (2022) and Roshani et al. (2023). Through this comparison, it is clear that the proposed diplexer has a good performance, compact size, lowest FBW, low ILs, and high isolation.

5. Conclusion

A novel microstrip diplexer based on the DOSLR is presented and well-organized in this paper. The proposed research clarifies the properties and behavior of the design which is distinguished from other designs by very high power efficiency, high isolation, low ILs in dual bands, and very compact size. The dual cell structure depends on two BPFs and is improved by dual finger cells upper and lower feed lines Also, it progresses the isolation results as calculated by 35 dB for the 8.4 GHz band and 60 dB for the 10.8 GHz band, as well as the simulated IL for each band 0.4 dB/0.3 dB, respectively, with a fractional bandwidth of 2 and 4 % for each band. At the most, the proposed diplexer is designed to operate to serve 5 G applications in wide bands. In the end, the design is fabricated and

measured in lap by a Rohde and Schwarz analyzer to prove the comparison between the simulated and real fabrication with a very good agreement between them.

Author credit statement

Islam F. Abu Elkhair: conception and design of the work, data collection and tools, data analysis, methodology, software work, measurements, reporting and plotting the results, and drafting of the article. Hamdi A. Elmikati: project administration, supervision, and final approval of the version to be published. Mohamed M. Ashour: supervision, checking for grammar and plagiarism, and writing and publishing layout. Amr H. Hussein: conception and design of the work, review and investigation of the results, advice to improve results, supervision, methodology, providing resources, and critical revision of the article.

Conflicts of interest

None declared.

References

Alnagar, I.A., Mahmoud, N.M., Khames, S.A., Hussein, A.H., 2022. Efficient microstrip diplexer employing a new structure of dual-mode bandpass filter. Am Sci Res J Eng Technol Sci 88, 68–76.

Bavandpour, S.K., Roshani, S., Pirasteh, A., Roshani, S., Seyedi, H., 2021. A compact lowpass − dual bandpass diplexer with high output ports isolation. AEU Int J Electr Commun 135, 153–748.

Ben Haddi, S., Zugari, A., Zakriti, A., El Ouahabi, M., El Khamlichi, D., 2023. Compact microstrip diplexer design using new octagonal resonators for 5G and Wi-Fi applications. J. Instrum. 18, 3–33.

Bui, D.H.N., Vuong, T.P., Allard, B., Verdier, J., Benech, P., 2017. Compact low-loss microstrip diplexer for RF energy harvesting. Electron. Lett. 53, 552–554.

Chaudhary, M.A., Roshani, S., Shabani, S., 2023. A miniaturized dual-band diplexer design with high port isolation for UHF/SHF applications using a neural network model. Micromachines 14, 849.

Chinig, A., Bennis, H., 2017. A novel design of an H-shaped microstrip diplexer. J Microw Optoelectron Electromag Appl 16, 966–981.

Chinig, A., Zbitou, J., Errkik, A., Elabdellaoui, L., Tajmouati, A., 2014. A new microstrip diplexer using open-loop resonators. J Microw Optoelectron Electromag Appl 13, 185–196.

Chinig, A., Errkik, A., Abdellaoui, LEl, Tajmouati, A., 2016. Design of a microstrip diplexer and triplexer using open loop resonators. J Microw Optoelectron Electromagn Appl 15, 65–80.

Chuang, M.-L., Wu, M.-T., 2011. Microstrip diplexer design using common T-shaped resonator. IEEE Microw. Wireless Compon. Lett. 21, 583–585.

Dembele, S.N., Bao, J., Zhang, T., Bukuru, D., 2019. Compact microstrip diplexer based on dual closed loop stepped impedance resonator. Prog. Electromagn. Res. 89, 233–241.

Farah, M.C., Salah-Belkhodja, F., Khelil, K., 2022. A design of a compact microwave diplexer in microstrip technology based on bandpass filters using stepped impedance resonator. J Microw Optoelectron Electromagn Appl 21, 242–264.

Gorur, A.K., Turkeli, A., Buyuktuna, M., Dogan, E., Karpuz, C., Gorur, A., 2022. A high isolation quad-channel microstrip diplexer based on codirectional split ring resonators. Microw. Opt. Technol. Lett. 64, 1382–1386.

Haddi, S.B., Zugari, A., Zakriti, A., Achraou, S., 2022. High isolation microstrip bandpass diplexer for industry 4.0 communication. Microsyst. Technol. 28, 1167–1178.

Hammed, R.T., 2022. Multilayered U-shape diplexer for high performance multifunctional wireless communication systems. AEU Int J Electr Comm 150, 154–217.

Hassan, A.Y., Hagag, M.F., Abdel Aziz, A.A., Abdalla, M.A., 2021. A compact diplexer using coupled π-CRLH zeroth resonators. IETE J. Res. 69, 1–8.

Roshani, S., Yahya, S.I., Mezaal, Y.S., Roshani, S., 2023. Design of a compact quad-channel microstrip diplexer for L and S band applications. Micromachines 14, 553.

Song, K, Ding, X, Zhu, L, Jin, S, Fan, Y, 2023. Optimization technology of the microwave diplexer based on spatial mapping algorithm. IEEE Trans Circuits Syst II 70, 1.

Tahmasbi, M., Razaghian, F., Roshani, S., 2021. Design of bandpass–bandpass diplexers using rectangular-, T-, and L-shaped resonators for hybrid power amplifier and 5G applications. Analog Integr. Circuits Signal Process. 109, 585–597.

Wu, Y., Hao, L., Wang, W., Yang, Y., 2022. Miniaturized and low insertion loss diplexer using novel inter-digital capacitors and microstrip section inductors. IEEE Trans Circuits Systems II 69, 4303–4307.

Yang, Y., Yu, M., Wu, Q., Zeng, Y., 2019. Tunable diplexer design with redundant coupling. IEEE Trans. Microw. Theor. Tech. 67, 4976–4983.

Zhang, P., Weng, M.-H., Yang, R.-Y., 2021. A compact wideband diplexer using stub-loaded square ring resonators. Electromagnetics 41, 167–184.

Zhou, L., Zhou, W., Sun, Y., Han, Y., Jiang, J., Zhang, D., 2023. Design of high-order resonator HTS diplexer with very different FBW. Electronics 12, 691.